Purdue University

Purdue e-Pubs

5-19-2014

Time-dependent density functional theory of coupled electronic lattice motion in quasi-two-dimensional crystals

Vladimir U. Nazarov
Academia Sinica - Taiwan, Qatar Foundation

Fhhad Alharbi
Qatar Foundation, King Abdulaziz City for Science and Technology

Timothy Fisher
Purdue University, Birck Nanotechnology Center, tsfisher@purdue.edu

Sabre Kais
Purdue University, Birck Nanotechnology Center, kais@purdue.edu

Follow this and additional works at: https://docs.lib.purdue.edu/nanopub

Part of the Nanoscience and Nanotechnology Commons

Time-dependent density functional theory of coupled electronic lattice motion in quasi-two-dimensional crystals

Vladimir U. Nazarov,[1,2,*] Fahhad Alharbi,[3,2] Timothy S. Fisher,[4,2] and Sabre Kais[5,2]

[1]*Research Center for Applied Sciences, Academia Sinica, Taipei 11529, Taiwan*
[2]*Qatar Environment and Energy Research Institute, Qatar Foundation, Doha, Qatar*
[3]*King Abdulaziz City for Science and Technology, Riyadh, Saudi Arabia*
[4]*Birck Nanotechnology Center and School of Mechanical Engineering, Purdue University, West Lafayette, Indiana 47906, USA*
[5]*Department of Chemistry, Physics and Birck Nanotechnology Center, Purdue University, West Lafayette, Indiana 47907, USA*

Electron-holes, phonons, and plasmons come in close proximity to each other in the low-energy range of the excitation spectrum of two-dimensional (2D) crystals, breaking the validity of the weakly interacting-quasiparticles picture. By including the lattice oscillations into the scheme of time-dependent density-functional theory, we open a pathway to the *ab initio* treatment of the coupled low-energy excitations in 2D crystals. With the use of graphene as an important test system, we find the strong coupling of the elementary excitations, giving rise to new hybrid collective modes. The total (including both the electronic and ionic response) dielectric function $\varepsilon_{\text{tot}}(\omega)$ is constructed and the picture of the low-energy excitation spectrum of graphene is redrawn.

PACS number(s): 73.22.Pr, 63.22.Rc, 73.20.Mf

I. INTRODUCTION

The concept of elementary excitations has proven exceptionally fruitful in solid-state physics, allowing the reduction of the motion of interacting particles to that of independent quasiparticles [1]. More realistically, the quasiparticles may interact, although preserving their individuality provided the interaction is weak. An important counterexample realizes in graphene—a two-dimensional (2D) crystal comprised of a honeycomb lattice of carbon atoms [2]—where, in the energy range up to a few hundred meV, the electron-hole, phonon, and plasmon spectra overlap, suggesting the strong interaction between those elementary excitations [3–11]. The interplay of quasiparticles is of fundamental importance in understanding the electronic and lattice properties of 2D crystals [3], as well as the superconductivity in 2D materials [12–14], and the 2D heat transfer, to name only a few.

The density-functional perturbation theory (DFPT) [15], which is an established method of the *ab initio* adiabatic treatment of phonons, fundamentally fails in capturing the dynamical nature of the coupled plasmon-phonon oscillations. In this paper, by the use of time-dependent density-functional theory (TDDFT), we develop and implement the fully *dynamic* approach, thus fulfilling the program of the *ab initio* inclusion of the interaction between the electron-hole, plasmon, and phonon excitations on the equal footing [3]. We find the strong coupling between the recently predicted low-energy collective excitations of the electronic subsystem [16,17] and phonons, which dramatically changes the spectrum of graphene, leading to the birth of new hybrid excitation modes.

The organization of this paper is as follows. In Sec. II we reproduce and discuss results of the *uncoupled* electron and phonon motion in 2D crystals. The controversial issue of the existence of the acoustic plasmon in graphene is also analyzed in that section and Appendix B. In Sec. III and Appendix C, we construct the TDDFT formalism of the cou-

pled electronic-phononic motion in the linear (with respect to the external field) response regime. In Sec. IV, we present and discuss results of numerical calculations and draw conclusions derived from the latter. In Appendix A we give a solution to an important technical problem of retrieving the dielectric response of a stand-alone 2D crystal from the results of the 3D supercell calculation. In Appendix D we give the derivation of the total (including both the electronic and ionic degrees of freedom) dielectric function of a 2D crystal. In Appendix E we compare with the available experimental data and with the case of the static coupling.

II. ELECTRONIC AND PHONONIC EXCITATIONS IN GRAPHENE

We start by presenting results of calculations of the low-energy electronic and phononic spectra of graphene without the coupling between the two subsystems. To make the problem treatable, we use the supercell method, building a fictitious 3D system by the periodic replication of the quasi-2D crystal with the separation d between the layers. It is, however, known that whatever large d is, for sufficiently small wave vector q, the layers interact electrodynamically, making the results for the substitute 3D system irrelevant to the stand-alone 2D crystal of interest [18]. We overcome this difficulty quite generally, expressing the 3D dielectric function of the substitute system via the 2D dielectric function of the original one with account of the interaction between the layers, and then inverting the problem. This results in the relation (see Appendix A)

$$\frac{1}{\varepsilon_{2D}(\mathbf{q},\omega)} = 1 + \frac{1}{2}\frac{1}{\left[\frac{1}{\varepsilon_{3D}(\mathbf{q},\omega;d)}-1\right]qd + \frac{1}{e^{qd}-1}}, \quad (1)$$

where $\mathbf{q}$ and ω are the wave vector and the frequency, respectively, of the laterally applied electric field, and $\varepsilon_{3D}(\mathbf{q},\omega;d)$ is the dielectric function of the substitute 3D system. The left-hand side of Eq. (1) does not depend on d, in accordance
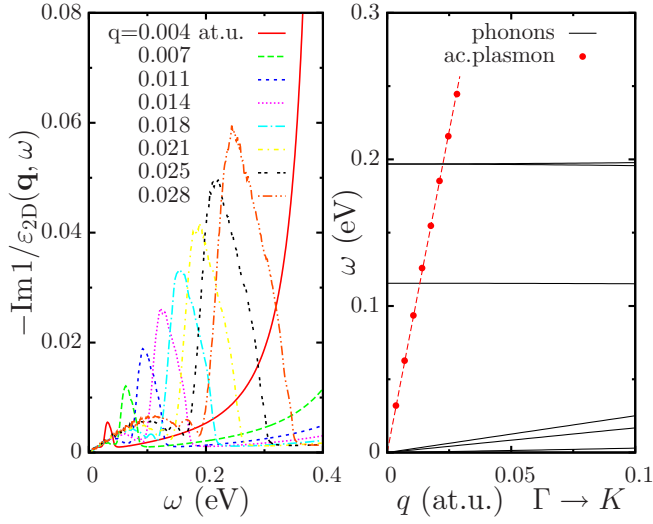
---

*nazarov@gate.sinica.edu.tw

FIG. 1. (Color online) Left: Energy-loss function of the mono-layer graphene doped with 1.2×10^{14} cm^{-2} electrons corresponding to the Fermi energy shift up by 1 eV. Plasmon peaks with linear (acoustic) dispersion are dominant in the low-frequency range of the spectra. The variation of $\mathbf{q}$ is along the ΓK direction. Right: Dispersion of phonons (black solid lines). From bottom to top: three acoustic phonons, z-polarized optical phonon, two xy-polarized optical phonons, and acoustic plasmon (red symbols) dispersion. The red dashed line is the linear best fit to the acoustic plasmon.

with the fact that it is a true characteristic of the stand-alone 2D crystal.

Our numerical calculations for the doped monolayer graphene employ the full-potential linear augmented plane-wave (FP-LAPW) code Elk [19]. The local-density approximation to the exchange-correlation (xc) potential [20] was used [21]. We have carried out calculations with $d = 30$, 60, and 100 a.u., producing, after the use of Eq. (1), practically identical results.

In Fig. 1, left panel, the energy-loss function of graphene is plotted for a number of equidistant values of the wave vector. The calculation with the carbon atoms fixed at their equilibrium positions has been used at this stage. The acoustic plasmon [22] can be easily recognized by the linear dispersion of the peak with the wave vector, which is in qualitative agreement with the recent findings obtained with the use of the pseudopotential method [16,17]. In Fig. 1, right panel, we plot the phonon spectra of graphene obtained by DFPT together with the acoustic plasmon dispersion derived from the energy-loss function in the left panel. Acoustic plasmon and optical phonons dispersion curves intersect, which suggests their interaction and constitutes the motivation for the study of the coupled modes.

III. COUPLED PLASMON-PHONON MODES

We treat the problem of coupled plasmon-phonon oscillations within the *dynamic* (frequency-dependent) linear-response theory for both electrons and ions: self-consistently, ions are driven by an external probing ac electric field and the Coulomb field of moving electrons, and, in turn, electrons

move under the action of the external field and the dynamic field of moving ions. Our goal is to put the coupled electron-ion motion in terms of the density-response function $\chi(\mathbf{r},\mathbf{r}',\omega)$ [or equivalently, the nonlocal dielectric function $\varepsilon(\mathbf{r},\mathbf{r}',\omega)$] of the 2D crystal with *ions at rest* in their equilibrium positions and the dynamic matrices [15] D of the lattice.

We consider an infinite quasi-2D crystal lying in the xy plane. The 2D lattice vectors are denoted by $\mathbf{R}$, while the position of the αth atom within the unit cell is $\mathbf{b}_\alpha$. A weak external potential of the form

$$\delta\phi^{\text{ext}}(\mathbf{r},t) = \delta\phi^{\text{ext}}(\mathbf{q},z,\omega)e^{i(\mathbf{q}\cdot\mathbf{r}-\omega t)} \quad (2)$$

is applied to the system, where $\mathbf{r}$ is the 3D position coordinate vector and $\mathbf{q}$ is the 2D wave vector. We seek for the response *including the ionic oscillations* around their equilibrium positions with the displacements given by

$$\mathbf{u}_{\alpha\mathbf{R}}(t) = \mathbf{u}_{\alpha\mathbf{R}}(\omega)e^{-i\omega t} = \mathbf{e}_\alpha(\omega)e^{i(\mathbf{q}\cdot\mathbf{R}-\omega t)} \quad (3)$$

with 3D amplitude vectors $\mathbf{e}_\alpha$. The total Coulomb potential in the system is

$$\phi(\mathbf{r},t) = \phi_0(\mathbf{r}) + \delta\phi(\mathbf{r},\omega)e^{-i\omega t}, \quad (4)$$

where ϕ_0 is the ground-state Coulomb potential and $\delta\phi$ is its first-order perturbation. The force experienced by the αth ion in the $\mathbf{R}$th unit cell is

$$\mathbf{F}_{\alpha\mathbf{R}}(t) = -Z_\alpha \nabla\phi_{\alpha\mathbf{R}}^{\text{eff}}(\mathbf{r},t)\big|_{\mathbf{r}=\mathbf{b}_\alpha+\mathbf{u}_{\alpha\mathbf{R}}(t)+\mathbf{R}}, \quad (5)$$

where Z_α is the charge of the αth ion in the unit cell and $\phi_{\alpha\mathbf{R}}^{\text{eff}}$ is the total Coulomb potential minus the self-interaction of the $(\alpha\mathbf{R})$th ion,

$$\phi_{\alpha\mathbf{R}}^{\text{eff}}(\mathbf{r},t) = \phi(\mathbf{r},t) - \frac{Z_\alpha}{|\mathbf{r} - \mathbf{b}_\alpha - \mathbf{u}_{\alpha\mathbf{R}}(t) - \mathbf{R}|}. \quad (6)$$

Expansion of Eq. (6) to the first order in the perturbation gives

$$\phi_{\alpha\mathbf{R}}^{\text{eff}}(\mathbf{r},t) = \phi_0(\mathbf{r}) - \frac{Z_\alpha}{|\mathbf{r} - \mathbf{b}_\alpha - \mathbf{R}|} + \delta\phi(\mathbf{r},\omega)e^{-i\omega t}$$
$$+ \mathbf{u}_{\alpha\mathbf{R}}(t) \cdot \nabla \frac{Z_\alpha}{|\mathbf{r} - \mathbf{b}_\alpha - \mathbf{R}|}. \quad (7)$$

Further, since

$$\phi_0(\mathbf{r}) = v^{\text{ext}}(\mathbf{r}) - \int \frac{n_0(\mathbf{r}')}{|\mathbf{r} - \mathbf{r}'|}d\mathbf{r}', \quad (8)$$

where $n_0(\mathbf{r})$ is the ground-state electron particle density and $v^{\text{ext}}(\mathbf{r})$ is the equilibrium ions' potential

$$v^{\text{ext}}(\mathbf{r}) = \sum_{\beta\mathbf{R}} \frac{Z_\beta}{|\mathbf{r} - \mathbf{b}_\beta - \mathbf{R}|}, \quad (9)$$

we can write for the force acting on the αth ion in the **0**th cell

$$\mathbf{F}_\alpha(\omega) = -Z_\alpha \left\{ [\mathbf{e}_\alpha(\omega) \cdot \nabla] \nabla \left[\sum_{(\beta\mathbf{R})\neq(\alpha\mathbf{0})} \frac{Z_\beta}{|\mathbf{r} - \mathbf{b}_\beta - \mathbf{R}|} \right. \right.$$
$$\left. \left. - \int \frac{n_0(\mathbf{r}')}{|\mathbf{r} - \mathbf{r}'|}d\mathbf{r}' \right] + \nabla\delta\phi_{\alpha\mathbf{0}}^{\text{eff}}(\mathbf{r},\omega) \right\}_{\mathbf{r}=\mathbf{b}_\alpha}, \quad (10)$$

where the corresponding zeroth order term has been set to zero because ions are in their equilibrium positions in the

crystal's ground state. The electronic response is governed by the equation

$$\delta\phi^{\text{ext}}(\mathbf{r},t) + \delta\phi^I_b(\mathbf{r},t) = \int \varepsilon(\mathbf{r},\mathbf{r}',t-t')\delta\phi(\mathbf{r}',t')d\mathbf{r}'dt', \quad (11)$$

where

$$\delta\phi^I_b(\mathbf{r},t) = -\sum_{\alpha\mathbf{R}} \mathbf{u}_{\alpha\mathbf{R}}(t) \cdot \nabla \frac{Z_\alpha}{|\mathbf{r} - \mathbf{b}_\alpha - \mathbf{R}|} \quad (12)$$

is the ionic displacement bare potential and ε is the nonlocal dielectric function of the ideal (ions at rest at equilibrium) crystal.

Based on Eqs. (5) and (7)–(12), a rather lengthy although straightforward algebra (see Appendix C) leads to the following expression for the force:

$$F_{\alpha i}(\mathbf{q},\omega) = F^{\text{ext}}_{\alpha i}(\mathbf{q},\omega) + F^{ei}_{\alpha i}(\mathbf{q},\omega) - \sum_{\beta k} D_{\alpha i,\beta k}(\mathbf{q})e_{\beta k}(\omega)$$

$$+ \sum_{\beta k} \left[Q_{\alpha i,\beta k}(\mathbf{q},\omega) - Q_{\alpha i,\beta k}(\mathbf{q},0) \right] e_{\beta k}(\omega), \quad (13)$$

where $D_{\alpha i,\beta k}$ are the so called dynamic matrices [23] of the conventional DFPT [15] and

$$F^{\text{ext}}_{\alpha i}(\mathbf{q},\omega) = -Z_\alpha \sum_{\mathbf{G}} e^{i(\mathbf{G}+\mathbf{q})\cdot\mathbf{b}_\alpha}$$

$$\times \left[i(G_i + q_i) + \hat{z}_i \frac{\partial}{\partial z} \right] \phi^{\text{ext}}(\mathbf{G}+\mathbf{q},z,\omega) \Bigg|_{z=0}, \quad (14)$$

$$F^{ei}_{\alpha i}(\omega) = 2\pi i Z_\alpha \sum_{\mathbf{GG}'} \int Y_i(\mathbf{G}+\mathbf{q},z)\chi_{\mathbf{GG}'}(\mathbf{q},z,z',\omega)$$

$$\times e^{i(\mathbf{G}+\mathbf{q})\cdot\mathbf{b}_\alpha} \phi^{\text{ext}}(\mathbf{G}'+\mathbf{q},z',\omega)dz\,dz', \quad (15)$$

$$Q_{\alpha i,\beta k}(\mathbf{q},\omega) = -\frac{(2\pi)^2}{s_0} \sum_{\mathbf{GG}'} Z_\alpha Z_\beta e^{i(\mathbf{G}+\mathbf{q})\cdot\mathbf{b}_\alpha} e^{-i(\mathbf{G}'+\mathbf{q})\cdot\mathbf{b}_\beta}$$

$$\times \int Y_i(\mathbf{G}+\mathbf{q},z)\chi_{\mathbf{GG}'}(\mathbf{q},z,z',\omega)Y_k$$

$$\times (\mathbf{G}'+\mathbf{q},z')dz\,dz', \quad (16)$$

where $\chi_{\mathbf{GG}'}$ is the interacting-particles density-response function of the ideal crystal, s_0 is the area of the unit cell, the vector function $\mathbf{Y}$ is defined as

$$\mathbf{Y}(\mathbf{p},z) = -e^{-p|z|}[\hat{\mathbf{p}} + i\hat{\mathbf{z}}\,\text{sgn}(z)], \quad (17)$$

and hat above a vector denotes a unit vector in the corresponding direction.

In Eq. (13), the first two terms are due to the dynamically screened external force in the ideal crystal and the third term is the statically screened restoring force of the displacement of the ions. The fourth term contains all the effects responsible for dynamic electron-phonon interaction. Obviously, with the neglect of the latter ($\omega = 0$ in the fourth term), Eq. (13) reduces to the conventional static DFPT case [15].

With the use of Eq. (3), Newton's law gives for the αth nucleus at the **0**th unit cell

$$-M_\alpha\omega^2\mathbf{e}_\alpha = \mathbf{F}_\alpha. \quad (18)$$

Equations (13)–(18) form a $3N$ system of linear equations for $3N$ unknowns $e_{\alpha,i}$, $i = 1,2,3$, where N is the number of atoms in the unit cell.

Once $\mathbf{e}_\alpha$ are found, the total 2D charge density is determined as (see Appendix D)

$$\delta\rho^{\text{tot}}_{2D}(\mathbf{q},\omega) = \delta\rho^I_{2D,b}(\mathbf{q},\omega) + \sum_{\mathbf{G}'} \int \chi_{0\mathbf{G}'}(\mathbf{q},z,z',\omega)$$

$$\times [\delta\phi^{\text{ext}}(\mathbf{G}'+\mathbf{q},z',\omega)+\delta\phi^I_b(\mathbf{G}'+\mathbf{q},z',\omega)]dz\,dz', \quad (19)$$

where $\delta\rho^I_{2D,b}$ is the bare charge perturbation due to the ions' motion. Equation (19) enables us to obtain the total 2D density-response function $\chi^{\text{tot}}_{2D}(\mathbf{q},\omega)$, and the total dielectric function is then found by the equation

$$\frac{1}{\varepsilon^{\text{tot}}_{2D}(\mathbf{q},\omega)} = 1 + \frac{2\pi}{q} \chi^{\text{tot}}_{2D}(\mathbf{q},\omega). \quad (20)$$

Importantly, the energy exchange between the electronic and ionic subsystems occurs as a result of their coupled motion. The energy given away by ions to electrons per unit cell per unit time is

$$W = -\frac{\omega}{2} \sum_\alpha \text{Im} \left(\mathbf{F}^{\text{ext}}_\alpha \cdot \mathbf{e}^*_\alpha \right). \quad (21)$$

IV. RESULTS AND CONCLUSIONS

In Figs. 2 and 3, the total dielectric function of graphene is plotted and compared with that due to the response of the electronic subsystem only (frozen lattice). Clearly, the electronic excitations are strongly modified by those of the lattice whenever the former approach the energies of the acoustic and the xy-polarized optical phonons (pure phonons are shown by black vertical arrows) [24]. The same
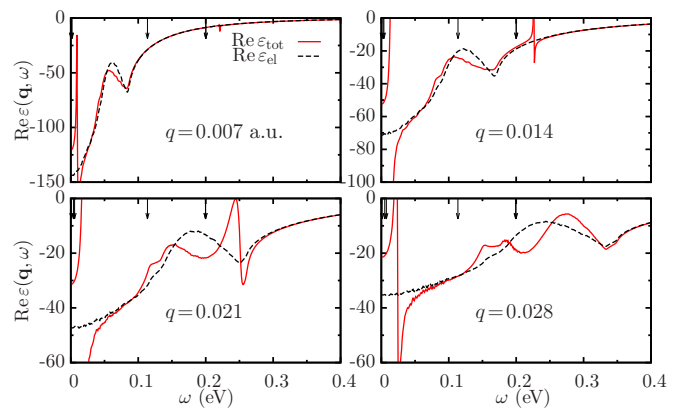

FIG. 2. (Color online) Real part of the total (including both the electronic and ionic response) dielectric function (red solid line) and its frozen-lattice counterpart (black dashed line). The calculation was carried out for monolayer graphene doped with 1.2×10^{14} cm^{-2} electrons corresponding to the Fermi energy shift up by 1 eV. Vertical black arrows show positions of uncoupled phonons.

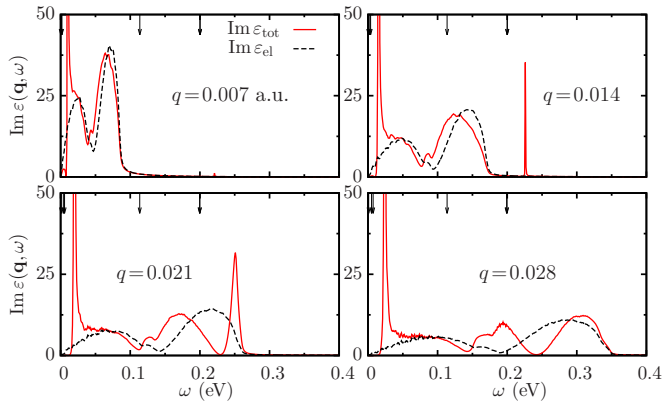FIG. 3. (Color online) Same as Fig. 2, but for the imaginary part of the dielectric function.

FIG. 5. Energy transfer per unit cell per unit time from the ionic to the electronic subsystem.

conclusions can be made by considering the total energy-loss function plotted in Fig. 4. Interestingly, the coupling with the xy-polarized optical phonon leads to the splitting of both the absorption (Fig. 3) and the energy-loss (Fig. 4) peaks into two. High-intensity narrow low-energy peaks originate from acoustic phonons, acquiring a finite linewidth and experiencing a considerable blueshift due to the coupling with electrons.

In Fig. 5, we plot the energy transferred per unit cell per unit time from the ionic to the electronic subsystem of monolayer graphene calculated by Eq. (21). We anticipate that the process of the electrons heating by the ionic lattice will be experimentally observable in two-terminal suspended graphene experiments. For example, Yiğen *et al.* [25] recently demonstrated the ability to distinguish electronic from phononic heat conduction in a self-heated suspended device. The associated analysis of electron-phonon scattering did not, however, include plasmonic effects, which would be observable at moderate temperatures and under ac fields near the resonances predicted here. Here it must be also reemphasized that thorough understanding of plasmons-phonons interactions is particularly important in the field of superconductivity [26].

It must be noted that the advance of this work has been possible to make owing to the simultaneous resolution of the

two major problems: (i) nonadiabatic inclusion of the ions' motion into the scheme of the TDDFT and (ii) isolation of the dielectric response of a *stand alone* quasi-2D crystal, achieved by the elimination of the interaction between copies of the crystal in the fictitious periodic array of the supercell geometry. In our formalism, the motion of neither electrons nor ions is confined to the mathematical plane, which, if otherwise, would be a 2D model. Therefore, the results are obtained within the full quasi-2D approach. Regarding our use of the integrated in z-direction functions such as L_{2D} and ϵ_{2D}, it should be noted that (i) those can be ascribed the exact meaning in the quasi-2D case and (ii) while they are the convenient quantities to plot, results can be presented in other forms as, e.g., the frequency dependence of the ion's oscillation amplitudes, which is included as Fig. 6.

For the sake of completeness, in Fig. 7 we plot the energy-loss function of graphene at higher energies, where the 2D (sheet) plasmon [27,28] dominates the spectra. In this range, plasmon and phonons practically do not couple, as can be judged from the close coincidence of the results of calculations with and without electron-phonon interaction. Obviously, this is due to the relatively high frequency of the 2D plasmon oscillation, with which phonons cannot catch up.

In conclusion, we have developed a fully dynamic approach to coupled electron-lattice vibrations in quasi-two-dimensional crystals. By this, the electron-holes, phonons, and
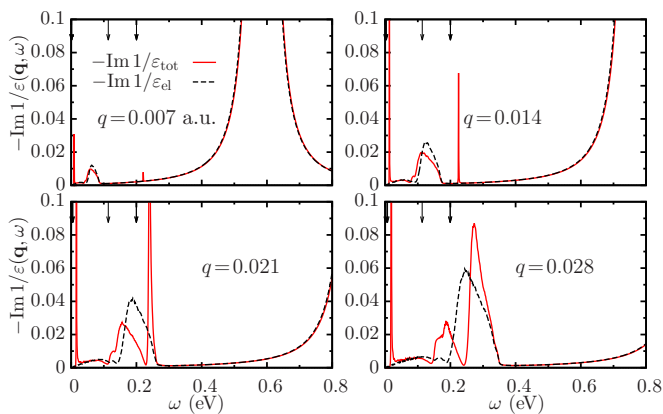

FIG. 4. (Color online) Same as Fig. 2, but for the 2D energy-loss function. The strong feature that does not fit into the plot is the 2D (sheet) plasmon which practically does not couple to phonons.
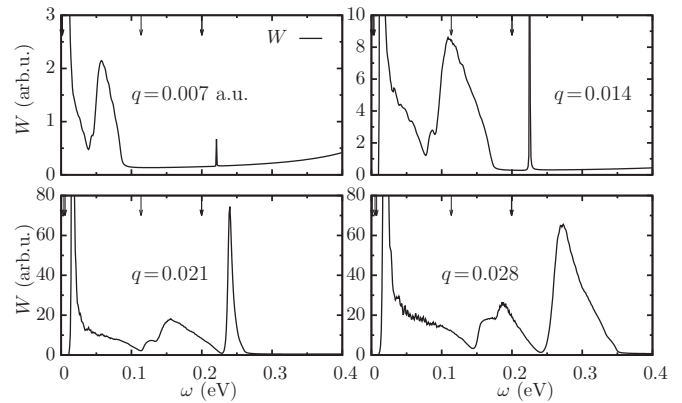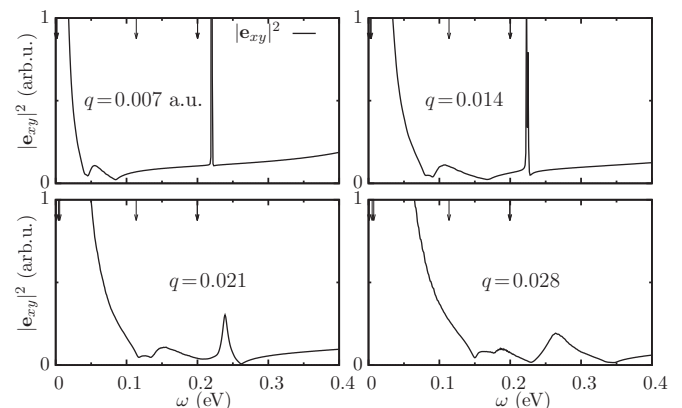

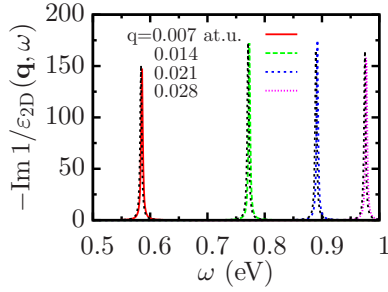FIG. 6. Ions' displacement amplitudes squared versus the frequency.

FIG. 7. (Color online) 2D energy-loss function within a higher energy range than in Fig. 4. The 2D (sheet) plasmon dominates this part of the spectra. The dotted black line represents the frozen-lattice calculation.

plasmons are dealt with on an equal footing, making the *ab initio* treatment of the low-lying excitation spectra feasible. The method has been applied to graphene, revealing the quite different behavior of the coupled modes compared with the individual phonons and plasmons. We have calculated the total wave-vector- and frequency-dependent dielectric function of graphene with an account of both the electronic and ionic degrees of freedom. The coupling which we found provides a mechanism for the transfer of energy between the electronic subsystem and the lattice. Promising pathways of the cooling of the lattice by the electronic subsystem can be clearly previewed.

APPENDIX A: 2D DIELECTRIC RESPONSE FROM A 3D SUPERCELL CALCULATION

Let us consider a periodic array of identical quasi-2D crystals with the period d. Let $\chi_{\mathbf{GG'}}(\mathbf{q},z,z',\omega)$ be the (interacting-particles) density-response function of a single quasi-2D crystal. The particle density induced in the vicinity of the zeroth quasi-2D crystal is

$$n_{\mathbf{G}}(\mathbf{q},z,\omega) = \sum_{\mathbf{G'}} \int \chi_{\mathbf{GG'}}(\mathbf{q},z,z',\omega) v_{\mathbf{G'}}^{\text{eff}}(\mathbf{q},z',\omega) dz', \quad \text{(A1)}$$

with

$$v_{\mathbf{G}}^{\text{eff}}(\mathbf{q},z,\omega) = v_{\mathbf{G}}^{\text{ext}}(\mathbf{q},z,\omega)$$
$$+ \frac{2\pi}{q}\delta_{\mathbf{G0}} \int_{-d/2}^{d/2} n_0(\mathbf{q},z',\omega) dz' \sum_{m=-\infty}^{\infty}{}' e^{-q|z-md|}, \quad \text{(A2)}$$

where the second term accounts for the influence of all $m \neq 0$ 2D crystals and the prime at the sum means that the $m = 0$ term is excluded from the summation. Equations (A1) and (A2)

yield

$$n_{\mathbf{G}}(\mathbf{q},z,\omega) = \sum_{\mathbf{G'}} \int \chi_{\mathbf{GG'}}(\mathbf{q},z,z',\omega) v_{\mathbf{G'}}^{\text{ext}}(\mathbf{q},z',\omega) dz'$$
$$+ \frac{4\pi n_0^{\text{2D}}(\mathbf{q},\omega)}{q(e^{qd}-1)} \int \chi_{\mathbf{G0}}(\mathbf{q},z,z',\omega)\cos(qz') dz', \quad \text{(A3)}$$

where

$$n_0^{\text{2D}}(\mathbf{q},\omega) = \frac{\sum_{\mathbf{G}} \int \chi_{\mathbf{0G}}(\mathbf{q},z,z',\omega) v_{\mathbf{G}}^{\text{ext}}(\mathbf{q},z',\omega) dz\, dz'}{1 - \frac{4\pi}{q(e^{qd}-1)} \int \chi_{\mathbf{00}}(\mathbf{q},z,z',\omega)\cos(qz') dz\, dz'} \quad \text{(A4)}$$

is the zeroth Fourier coefficient of the 2D particle density. In Eqs. (A3) and (A4) we can safely put $\cos(qz')$ to 1, since we are in the regime when $qa \ll 1$, where a is the z-direction width of the quasi-2D crystal. Then by Eqs. (A3) and (A4) and using the definition of the density-response function of the array system, which we denote by $\tilde{\chi}$, we can write

$$\tilde{\chi}_{\mathbf{G}g,\mathbf{G'}g'}(\mathbf{q},\omega) = \chi_{\mathbf{G}g,\mathbf{G'}g'}(\mathbf{q},\omega) + \frac{\chi_{\mathbf{G}g,\mathbf{00}}(\mathbf{q},\omega)\chi_{\mathbf{00},\mathbf{G'}g'}(\mathbf{q},\omega)}{\frac{q(e^{qd}-1)}{4\pi d} - \chi_{\mathbf{00},\mathbf{00}}(\mathbf{q},\omega)}, \quad \text{(A5)}$$

where

$$\chi_{\mathbf{G}g,\mathbf{G'}g'}(\mathbf{q},\omega) = \frac{1}{d} \int \chi_{\mathbf{GG'}}(\mathbf{q},z,z',\omega) e^{i(g'z'-gz)} dz\, dz', \quad \text{(A6)}$$

and g's are the reciprocal vectors of the periodic array in z direction.

Equation (A5) can be inverted to express the density-response function χ of the single quasi-2D crystal through $\tilde{\chi}$—the density-response function of the array of such crystals. Setting all indices to zero in Eq. (A5) and resolving in respect to $\chi_{\mathbf{00},\mathbf{00}}$, we have

$$\chi_{\mathbf{00},\mathbf{00}}(\mathbf{q},\omega) = \frac{\tilde{\chi}_{\mathbf{00},\mathbf{00}}(\mathbf{q},\omega)}{1 + \frac{4\pi d}{q(e^{qd}-1)}\tilde{\chi}_{\mathbf{00},\mathbf{00}}(\mathbf{q},\omega)}. \quad \text{(A7)}$$

Then setting $(\mathbf{G'}g') = (\mathbf{0}0)$ in Eq. (A5), we have the first of the Eqs. (A8)

$$\chi_{\mathbf{G}g,\mathbf{00}}(\mathbf{q},\omega) = \left[1 - \frac{4\pi d}{q(e^{qd}-1)}\chi_{\mathbf{0000}}(\mathbf{q},\omega)\right]\tilde{\chi}_{\mathbf{G}g,\mathbf{00}}(\mathbf{q},\omega),$$
$$\chi_{\mathbf{00},\mathbf{G'}g'}(\mathbf{q},\omega) = \left[1 - \frac{4\pi d}{q(e^{qd}-1)}\chi_{\mathbf{00},\mathbf{00}}(\mathbf{q},\omega)\right]\tilde{\chi}_{\mathbf{00},\mathbf{G'}g'}(\mathbf{q},\omega),$$
$$\text{(A8)}$$

and similarly for the second of these equations. Finally, we write

$$\chi_{\mathbf{G}g,\mathbf{G'}g'}(\mathbf{q},\omega) = \tilde{\chi}_{\mathbf{G}g,\mathbf{G'}g'}(\mathbf{q},\omega) - \frac{\chi_{\mathbf{G}g,\mathbf{00}}(\mathbf{q},\omega)\chi_{\mathbf{00},\mathbf{G'}g'}(\mathbf{q},\omega)}{\frac{q(e^{qd}-1)}{4\pi d} - \chi_{\mathbf{00},\mathbf{00}}(\mathbf{q},\omega)}. \quad \text{(A9)}$$

Together, Eqs. (A9), (A8), and (A7) solve the problem of the isolation of the single 2D-crystal response from that of the surrounding members of the array.

For the dielectric functions we can write

$$\frac{1}{\tilde{\varepsilon}(\mathbf{q},\omega)} = 1 + \frac{4\pi}{q^2}\tilde{\chi}_{00,00}(\mathbf{q},\omega), \qquad (A10)$$

$$\frac{1}{\varepsilon_{2D}(\mathbf{q},\omega)} = 1 + \frac{2\pi d}{q}\chi_{00,00}(\mathbf{q},\omega). \qquad (A11)$$

With the use of Eqs. (A10), (A11), and (A7) we arrive at Eq. (1).

We conclude this section with a short discussion of the range of the applicability of Eqs. (1) and (A7)–(A9) and consider some limiting cases. First of all, d must be larger than the effective width of a quasi-2D crystal, i.e., the wave functions of two adjacent layers must not overlap. This constitutes only a weak lower bound on d, since $d \gtrsim 10$ a.u. usually already satisfies the requirement. Secondly, through this section we assume that $Gd \gg 1$ for all $\mathbf{G} \neq \mathbf{0}$, which ensures that all the harmonics of the field but the zeroth die out on the distance from one layer to another. The restriction this imposes is approximately the same as the previous one. With the above two requirements satisfied, Eqs. (1) and (A7)–(A9) are valid with no additional restriction on the lower bound of q.

For $qd \gg 1$, Eq. (1) reduces to

$$\frac{1}{\varepsilon_{2D}(\mathbf{q},\omega)} = 1 + \frac{qd}{2}\left[\frac{1}{\varepsilon_{3D}(\mathbf{q},\omega;d)} - 1\right], \qquad (A12)$$

which can be easily understood in terms of an array of noninteracting sheets of the density n_{2D} comprising the 3D density $n_{3D} = n_{2D}/d$.

It must be noted that the derivation of this section has been carried out in terms of the *interacting-particles* density-response function χ and it does not rely on a particular relation between the latter and the Kohn-Sham independent-particles density-response function χ_s.

APPENDIX B: ACOUSTIC PLASMON IN GRAPHENE

There exists a controversy in the literature regarding the nature of the low-energy excitations in graphene. In Ref. [16], the excitation presented in our Fig. 1 has been identified as a plasmon. However, it was mistakenly given the name of "nonlinear plasmon", while we have shown that it has the linear (acoustic) dispersion at small wave vectors. The reason for the confusion was that the dispersion in Ref. [16] was studied starting from larger values of the wave vector, while referring to the dispersion law one usually means this at small (vanishing) wave vector (cf. the square root dispersion of the 2D sheet plasmon [27]). Note that no proof that the excitation is plasmon has been provided in Ref. [16].

On the other hand, in Ref. [17], this excitation has been identified as an acoustic plasmon. We, however, disagree with the definition of the 2D dielectric function adopted by the authors of that paper [Eq. (1) of Ref. [17]]. That definition has two obvious faults. (i) The sum in the right-hand side (RHS) of Eq. (1) is the 3D charge density at the point $z = 0$ rather than being the 2D charge density. Therefore, the multiplication of it by the 2D Coulomb potential makes no sense. And (ii), as a consequence of (i), the second term in the RHS of Eq. (1) is not dimensionless, while the first term is.
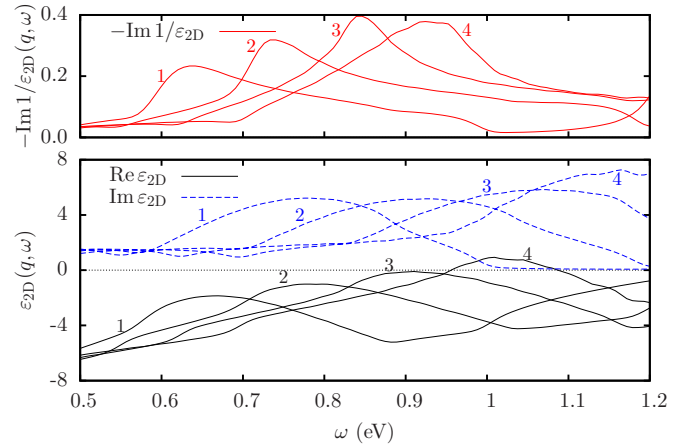

FIG. 8. (Color online) Evolution of the acoustic plasmon in graphene with the increase of the wave vector. Top: The energy-loss function $-\text{Im}\,1/\varepsilon_{2D}(q,\omega)$. Bottom: The dielectric function $\varepsilon_{2D}(q,\omega)$. Lines labeled 1, 2, 3, and 4 correspond to $q = 0.077, 0.092, 0.105,$ and 0.120 a.u., respectively.

It is, therefore, necessary to prove anew that the excitation in question, exhibiting the linear dispersion law, is a plasmon rather than, say, a single-particle excitation. In simple cases, it is usual to identify a peak at the energy-loss function as a plasmon if the real part of the dielectric function crosses zero at the same frequency. But what if $\text{Re}\,\varepsilon(q,\omega)$ comes close to the ω axis without crossing it? In Fig. 8, we plot the 2D dielectric function and the energy-loss function of graphene at larger values of q. For lines labeled with 4, we clearly deal with a plasmon since $\text{Re}\,\varepsilon$ crosses zero at $\omega \approx 0.95$ eV. For smaller q (lines labeled with 1, 2, and 3), $\text{Re}\,\varepsilon$ does not reach zero, although its modulus has minima. Clearly, peaks at the energy-loss function are associated with these minima, rather than with the maxima at $\text{Im}\,\varepsilon$, the latter contributing to the sloping right wings of the peaks at the energy-loss function. We, therefore, deal with plasmons in the 1, 2, and 3 cases as well, although mixed with single-particle transitions. The same situation is realized for smaller q in Fig. 1, as can be judged from Fig. 2, dashed black line, corresponding to the frozen-lattice calculation.

We note that in this more complicated situation than that with a pure plasmon characterized with the zero crossing by $\text{Re}\,\varepsilon$, the term of "acoustic plasmon" should be used with the clear understanding of the picture detailed above. Possibly, "linearly dispersed collective excitation" could make an alternative naming. We, however, stick to the first term believing that, used mindfully, it well conveys the essence of the matter.

APPENDIX C: DYNAMIC RESPONSE OF THE LATTICE: DERIVATION OF EQ. (13)

We perform the 2D Fourier transform of Eq. (12),

$$\delta\phi_b^I(\mathbf{G}+\mathbf{q},z,\omega) = \frac{2\pi i}{s_0}\sum_\alpha Z_\alpha \mathbf{e}_\alpha \cdot \mathbf{Y}(\mathbf{G}+\mathbf{q},z)e^{-i(\mathbf{G}+\mathbf{q})\cdot\mathbf{b}_\alpha},$$

$$(C1)$$

where the vector function $\mathbf{Y}$ is defined by Eq. (17). Inverting Eq. (11) in the reciprocal space, we can write

$$\delta\phi(\mathbf{G}+\mathbf{q},z,\omega) = \sum_{\mathbf{G}'} \int \varepsilon_{\mathbf{G}\mathbf{G}'}^{-1}(\mathbf{q},z,z',\omega)\left[\delta\phi^{\text{ext}}(\mathbf{G}'+\mathbf{q},z',\omega)+\delta\phi_b^I(\mathbf{G}'+\mathbf{q},z',\omega)\right]dz'. \tag{C2}$$

Then we can write for the gradient of the effective potential

$$\nabla\,\delta\phi_{\alpha\mathbf{0}}^{\text{eff}}(\mathbf{r},\omega)\Big|_{\mathbf{r}=\mathbf{b}_\alpha} = \sum_{\mathbf{G}\mathbf{G}'} e^{i(\mathbf{G}+\mathbf{q})\cdot\mathbf{b}_\alpha}\left[i(\mathbf{G}+\mathbf{q})+\hat{\mathbf{z}}\frac{\partial}{\partial z}\right]\int\Bigg\{\varepsilon_{\mathbf{G}\mathbf{G}'}^{-1}(\mathbf{q},z,z',\omega)\phi^{\text{ext}}(\mathbf{G}'+\mathbf{q},z',\omega)$$

$$+\frac{2\pi i}{s_0}\sum_\beta Z_\beta e^{-i(\mathbf{G}'+\mathbf{q})\cdot\mathbf{b}_\beta}\int\left[\varepsilon_{\mathbf{G}\mathbf{G}'}^{-1}(\mathbf{q},z,z',\omega)-\delta_{\mathbf{G}\mathbf{G}'}\delta(z-z')\right]\mathbf{e}_\beta\cdot\mathbf{Y}(\mathbf{G}'+\mathbf{q},z')\Bigg\}_{z=0}dz'$$

$$-\sum_{(\beta\mathbf{R})\neq(\alpha\mathbf{0})} e^{i\mathbf{q}\cdot\mathbf{R}}\nabla(\mathbf{e}_\beta\cdot\nabla)\frac{Z_\beta}{|\mathbf{r}-\mathbf{b}_\beta-\mathbf{R}|}\Bigg|_{\mathbf{r}=\mathbf{b}_\alpha}. \tag{C3}$$

We make use of the static sum rule [34]

$$\nabla n_0(\mathbf{r}) = -\int \chi(\mathbf{r},\mathbf{r}',0)\nabla' v^{\text{ext}}(\mathbf{r}')d\mathbf{r}'. \tag{C4}$$

Then

$$\int \frac{\nabla n_0(\mathbf{r}')}{|\mathbf{r}'-\mathbf{r}|}d\mathbf{r}' = \lim_{\mathbf{q}\to\mathbf{0}} \frac{2\pi i}{s_0}\sum_{\alpha\mathbf{G}\mathbf{G}'} Z_\alpha\int\left[\varepsilon_{\mathbf{G}\mathbf{G}'}^{-1}(\mathbf{q},z,z',0)-\delta_{\mathbf{G}\mathbf{G}'}\delta(z-z')\right]\mathbf{Y}(\mathbf{G}'+\mathbf{q},z')e^{i(\mathbf{G}+\mathbf{q})\cdot\mathbf{r}}e^{-i(\mathbf{G}'+\mathbf{q})\cdot\mathbf{b}_\alpha}dz'. \tag{C5}$$

Finally, we have for the force acting on the αth nucleus

$$F_{\alpha i} = F_{\alpha i}^{\text{ext}}(\mathbf{q},\omega) + F_{\alpha i}^{ei}(\mathbf{q},\omega) + \sum_{\beta k} N_{\alpha i,\beta k}(\mathbf{q},\omega)e_{\beta k}, \tag{C6}$$

$$N_{\alpha i,\beta k}(\mathbf{q},\omega) = P_{\alpha i,\beta k}(\mathbf{q},\omega) - \delta_{\alpha\beta}\sum_\gamma P_{\alpha i,\gamma k}(\mathbf{0},0), \tag{C7}$$

where

$$F_{\alpha i}^{\text{ext}} = -Z_\alpha\sum_{\mathbf{G}} e^{i(\mathbf{G}+\mathbf{q})\cdot\mathbf{b}_\alpha}\left[i(G_i+q_i)+\hat{z}_i\frac{\partial}{\partial z}\right]\phi^{\text{ext}}(\mathbf{G}+\mathbf{q},z,\omega)\Bigg|_{z=0}, \tag{C8}$$

$$F_{\alpha i}^{ei} = 2\pi Z_\alpha i\sum_{\mathbf{G}\mathbf{G}'}\int Y_i(\mathbf{G}+\mathbf{q},z)\chi_{\mathbf{G}\mathbf{G}'}(\mathbf{q},z,z',\omega)e^{i(\mathbf{G}+\mathbf{q})\cdot\mathbf{b}_\alpha}\phi^{\text{ext}}(\mathbf{G}'+\mathbf{q},z',\omega)dz\,dz', \tag{C9}$$

$$P_{\alpha i,\beta k}(\mathbf{q},\omega) = Q_{\alpha i,\beta k}(\mathbf{q},\omega) + S_{\alpha i,\beta k}(\mathbf{q}), \tag{C10}$$

$$Q_{\alpha i,\beta k}(\mathbf{q},\omega) = -\frac{(2\pi)^2}{s_0}\sum_{\mathbf{G}\mathbf{G}'} Z_\alpha Z_\beta e^{i(\mathbf{G}+\mathbf{q})\cdot\mathbf{b}_\alpha}e^{-i(\mathbf{G}'+\mathbf{q})\cdot\mathbf{b}_\beta}\int Y_i(\mathbf{G}+\mathbf{q},z)\chi_{\mathbf{G}\mathbf{G}'}(\mathbf{q},z,z',\omega)Y_k(\mathbf{G}'+\mathbf{q},z')dz\,dz', \tag{C11}$$

$$S_{\alpha i,\beta k}(\mathbf{q}) = \sum_{\mathbf{R}}[1-\delta_{\mathbf{R}\mathbf{0}}\delta_{\beta\alpha}]e^{i\mathbf{q}\cdot\mathbf{R}}\nabla_i\nabla_k\frac{Z_\alpha Z_\beta}{|\mathbf{r}-\mathbf{b}_\beta-\mathbf{R}|}\Bigg|_{\mathbf{r}=\mathbf{b}_\alpha}. \tag{C12}$$

Noting that within the static approximation ($\omega = 0$) our theory reduces to the conventional density-functional perturbation theory (DFPT) [15], we can conveniently rewrite Eq. (C6) as Eq. (13).

It is convenient for calculations to perform the following Fourier transforms

$$\chi_{\mathbf{G}\mathbf{G}'}(\mathbf{q},z,z',\omega) = \frac{1}{d}\sum_{gg'} \chi_{\mathbf{G}g\mathbf{G}'g'}(\mathbf{q},\omega)e^{i(gz-g'z')} \tag{C13}$$

into Eqs. (15) and (16). With the notation

$$\mathbf{Y}(\mathbf{p},g) = \int_{-d/2}^{d/2}\mathbf{Y}(\mathbf{p},z)e^{-igz}dz = -\frac{2}{g^2+p^2}\left\{\left[p+e^{-\frac{dp}{2}}\left(g\sin\frac{dg}{2}-p\cos\frac{dg}{2}\right)\right]\hat{\mathbf{p}}+\left[g-e^{-\frac{dp}{2}}\left(g\cos\frac{dg}{2}+p\sin\frac{dg}{2}\right)\right]\hat{\mathbf{z}}\right\},$$
$$\tag{C14}$$

we can write

$$F_{\alpha i}^{\text{ext}} = -i Z_\alpha \sum_{\mathbf{G}g} e^{i(\mathbf{G}+\mathbf{q})\cdot\mathbf{b}_\alpha} \left[G_i + q_i + \hat{z}_i g\right] \phi^{\text{ext}}(\mathbf{G}+\mathbf{q},g,\omega), \tag{C15}$$

$$F_{\alpha i}^{ei} = 2\pi i Z_\alpha \sum_{\mathbf{G}g\mathbf{G}'g'} e^{i(\mathbf{G}+\mathbf{q})\cdot\mathbf{b}_\alpha} Y_i(\mathbf{G}+\mathbf{q},-g)\chi_{\mathbf{G}g\mathbf{G}'g'}(\mathbf{q},\omega)\phi^{\text{ext}}(\mathbf{G}'+\mathbf{q},g',\omega), \tag{C16}$$

$$Q_{\alpha i,\beta k}(\mathbf{q},\omega) = -\frac{(2\pi)^2}{s_0 d} \sum_{\mathbf{G}g\mathbf{G}'g'} Z_\alpha Z_\beta e^{i(\mathbf{G}+\mathbf{q})\cdot\mathbf{b}_\alpha} e^{-i(\mathbf{G}'+\mathbf{q})\cdot\mathbf{b}_\beta} Y_i(\mathbf{G}+\mathbf{q},-g)\chi_{\mathbf{G}g\mathbf{G}'g'}(\mathbf{q},\omega)Y_k(\mathbf{G}'+\mathbf{q},g'). \tag{C17}$$

APPENDIX D: TOTAL DIELECTRIC FUNCTION

To find the total (including electron and ion subsystems motion) dielectric function, we write according to Eqs. (C2) and (C1)

$$\delta\rho_{2D}^{\text{tot}}(\mathbf{q},\omega) = d \sum_{\mathbf{G}'g'} \chi_{\mathbf{00G}'g'}(\mathbf{q},\omega)\big[\delta\phi^{\text{ext}}(\mathbf{G}'+\mathbf{q},g',\omega)$$
$$+ \delta\phi_b^I(\mathbf{G}'+\mathbf{q},g',\omega)\big] + \delta\rho_{2D,b}^I(\mathbf{q},\omega), \tag{D1}$$

where

$$\delta\phi_b^I(\mathbf{G}+\mathbf{q},g,\omega) = \frac{2\pi i}{s_0 d} \sum_\alpha Z_\alpha \mathbf{e}_\alpha \cdot \mathbf{Y}(\mathbf{G}+\mathbf{q},g)e^{-i(\mathbf{G}+\mathbf{q})\cdot\mathbf{b}_\alpha} \tag{D2}$$

and

$$\delta\rho_{2D,b}^I(\mathbf{G}+\mathbf{q},\omega) = -\frac{i}{s_0} \sum_\alpha Z_\alpha \mathbf{e}_\alpha \cdot (\mathbf{G}+\mathbf{q})e^{-i(\mathbf{G}+\mathbf{q})\cdot\mathbf{b}_\alpha}. \tag{D3}$$

APPENDIX E: COMPARISON WITH EXPERIMENT AND THE STATIC COUPLING

Reference [35] reports the electron energy-loss spectra (EELS) measurements for monolayer graphene deposited on SiC substrate. In Fig. 9 we plot a representative experimental

spectrum together with the results of our calculation with the parameters corresponding to the experiment. Since the doping level was not conclusively determined in Ref. [35], in our calculation we adjusted it by fitting the position of the 2D (sheet) plasmon (main feature in Fig. 9). The resulting value of the doping was 1.75×10^{13} cm^{-2}, which corresponds to the Fermi level shift by 0.4 eV. The influence of the substrate was included phenomenologically by the static dielectric function of SiC ($\varepsilon_\infty = 6.52$).

Comparing the theoretical and experimental results, we see that while the general trends are similar, quantitatively, with respect to both the peaks' position and the relative peaks' height, they are different. This, however, should not be surprising, considering that the influence of the substrate has been included within a much simplified model (ignoring its atomic structure).

Two more things must be said regarding the comparison between the theory and an EELS experiment. (i) The inelastic scattering of electrons in a reflection experiment is conventionally described by the so-called g function [36], which is defined as an amplitude of the outgoing e^{-qz} wave produced in response to the perturbation by the e^{qz} with unit amplitude. The g function is, therefore, a quantity different from the 2D energy-loss function, and to obtain it requires a separate calculation with the external field of $\phi_{\text{ext}}(\mathbf{r},t) = e^{qz}e^{i(\mathbf{q}\cdot\mathbf{r}-\omega t)}$. The theoretical curve in Fig. 9 is obtained with this new
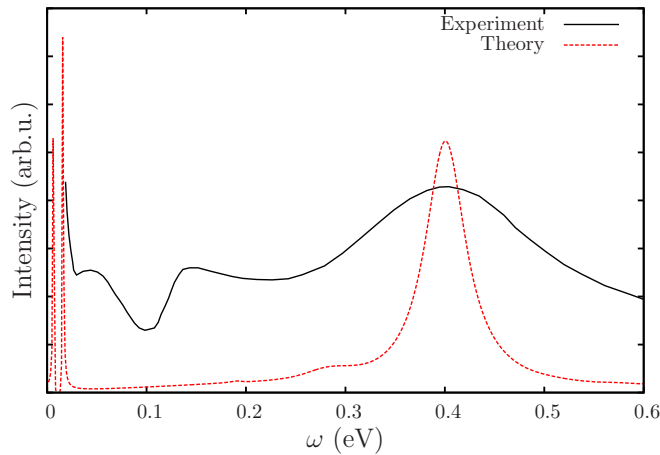

FIG. 9. (Color online) Experimental loss spectrum for 1 ML graphene grown on H-etched SiC(0001) for $q = 0.026$ a.u. [35] (black solid line) and our theory with account of the screening by the substrate (red dashed line).
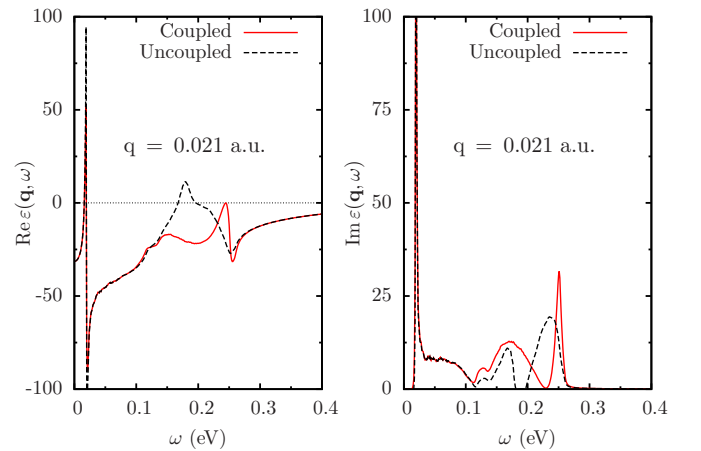

FIG. 10. (Color online) Total dielectric function of graphene with the full dynamic coupling of the electronic and phononic degrees of freedom (red solid line, labeled "Coupled") and that obtained without the last term in Eq. (13) (black dashed line, labeled "Uncoupled").

calculation. (ii) The description of the reflection EELS with the *g* function is valid only under the condition that the scattering of the incident electron takes place outside the electron density of the target (dipole scattering). Otherwise, for the impact scattering, a more involved technique must be used [37,38]. In our results in Fig. 9 we did not include the latter effects.

Summarizing, to conduct a conclusive comparison between the theory and experiment, EELS measurements on the stand-alone graphene will be necessary, and we believe that our work will motivate further experimental efforts.

Finally, let us consider the relationship with the uncoupled case. In Eq. (13), the last term is responsible for the dynamic coupling of the electronic and phononic degrees of freedom of 2D crystal. It is, therefore, instructive to compare results obtained with and without that term. In Fig. 10 we do this for graphene for $q = 0.021$ a.u., the difference clearly showing the importance of the dynamic coupling.

[1] D. Pines, *Elementary Excitations in Solids* (Perseus Books, Reading, MA, 1999).

[2] A. H. Castro Neto, F. Guinea, N. M. R. Peres, K. S. Novoselov, and A. K. Geim, Rev. Mod. Phys. **81**, 109 (2009).

[3] A. Bostwick, T. Ohta, T. Seyller, K. Horn, and E. Rotenberg, Nat. Phys. **3**, 36 (2007).

[4] W.-K. Tse and S. Das Sarma, Phys. Rev. Lett. **99**, 236802 (2007).

[5] C.-H. Park, F. Giustino, M. L. Cohen, and S. G. Louie, Phys. Rev. Lett. **99**, 086804 (2007).

[6] C.-H. Park, F. Giustino, M. L. Cohen, and S. G. Louie, Nano Lett. **9**, 1731 (2009).

[7] E. H. Hwang, R. Sensarma, and S. Das Sarma, Phys. Rev. B **82**, 195406 (2010).

[8] H. Yan, T. Low, W. Zhu, Y. Wu, M. Freitag, X. Li, F. Guinea, P. Avouris, and F. Xia, Nat. Photon. **7**, 394 (2013).

[9] M. Freitag, T. Low, W. Zhu, H. Yan, F. Xia, and P. Avouris, Nat. Commun. **4**, 1951 (2013).

[10] G.-Z. Kang, D.-S. Zhang, and J. Li, Phys. Rev. B **88**, 045113 (2013).

[11] A. Politano, V. Formoso, and G. Chiarello, J. Phys.: Condens. Matter **25**, 345303 (2013).

[12] Z. K. Tang, L. Zhang, N. Wang, X. X. Zhang, G. H. Wen, G. D. Li, J. N. Wang, C. T. Chan, and P. Sheng, Science **292**, 2462 (2001).

[13] M. Kociak, A. Y. Kasumov, S. Guéron, B. Reulet, I. I. Khodos, Y. B. Gorbatov, V. T. Volkov, L. Vaccarini, and H. Bouchiat, Phys. Rev. Lett. **86**, 2416 (2001).

[14] A. F. Hebard, M. J. Rosseinsky, R. C. Haddon, D. W. Murphy, S. H. Glarum, T. T. M. Palstra, A. P. Ramirez, and A. R. Kortan, Nature (London) **350**, 600 (1991).

[15] P. Giannozzi and S. Baroni, in *Handbook of Materials Modeling*, edited by S. Yip (Springer, New York, 2005), pp. 189–208.

[16] Y. Gao and Z. Yuan, Solid State Commun. **151**, 1009 (2011).

[17] M. Pisarra, A. Sindona, P. Riccardi, V. M. Silkin, and J. M. Pitarke, arXiv:1306.6273 [cond-mat.mes-hall].

[18] The problem of the interpretation of 3D supercell calculations for 2D systems is of general character, another notable example being the 2D scattering resonances unreproducible directly by the supercell method [29].

[19] http://elk.sourceforge.net

[20] J. P. Perdew and Y. Wang, Phys. Rev. B **45**, 13244 (1992).

[21] More advanced xc functionals including the recently developed one for the quasi-2D systems [30] could be used with our method. We, however, consider it methodologically preferential to first present these results with the use of the more conventional type of DFT.

[22] Acoustic plasmon is a plasmon exhibiting the linear dispersion with the wave vector [31], earlier known in metals with a surface state immersed in the bulk [32]. Recently, it has been experimentally observed [33] and confirmed theoretically [16, 17] in extrinsic (doped or gated) monolayer graphene. The identification of the acoustic plasmon has not been, however, conclusively settled so far, and in the Appendix B we, therefore, prove that this mode is plasmon indeed.

[23] In the context of this work, the conventional term dynamic matrices contains ambiguity since, in fact, they account exactly for the static (frequency independent) part of the force acting on an ion.

[24] The *z*-polarized optical phonon (almost) does not manifest itself in these spectra, because of the perturbation being applied laterally.

[25] S. Yiğen, V. Tayari, J. O. Island, J. M. Porter, and A. R. Champagne, Phys. Rev. B **87**, 241411(R) (2013).

[26] B. N. Ganguly and R. F. Wood, Phys. Rev. Lett. **28**, 681 (1972).

[27] F. Stern, Phys. Rev. Lett. **18**, 546 (1967).

[28] E. H. Hwang and S. Das Sarma, Phys. Rev. B **75**, 205418 (2007).

[29] V. U. Nazarov, E. E. Krasovskii, and V. M. Silkin, Phys. Rev. B **87**, 041405(R) (2013).

[30] L. Chiodo, L. A. Constantin, E. Fabiano, and F. Della Sala, Phys. Rev. Lett. **108**, 126402 (2012).

[31] D. Pines, Can. J. Phys. **34**, 1379 (1956).

[32] J. M. Pitarke, V. U. Nazarov, V. M. Silkin, E. V. Chulkov, E. Zaremba, and P. M. Echenique, Phys. Rev. B **70**, 205403 (2004).

[33] A. Politano, A. R. Marino, V. Formoso, D. Farías, R. Miranda, and G. Chiarello, Phys. Rev. B **84**, 033401 (2011).

[34] V. U. Nazarov, J. M. Pitarke, C. S. Kim, and Y. Takada, Phys. Rev. B **71**, 121106(R) (2005).

[35] C. Tegenkamp, H. Pfnür, T. Langer, J. Baringhaus, and H. W. Schumacher, J. Phys.: Condens. Matter **23**, 012001 (2011).

[36] A. Liebsch, *Electronic Excitations at Metal Surfaces* (Plenum, New York, 1997).

[37] V. U. Nazarov, Surf. Sci. **331–333**, 1157 (1995).

[38] V. U. Nazarov, Phys. Rev. B **59**, 9866 (1999).